Supplementary Information for

Nanostructures in TAGS thermoelectric materials induced by phase transitions associated with vacancy ordering

Thorsten Schröder,[†] Tobias Rosenthal,[†] Nadja Giesbrecht,[†] Markus Nentwig,[†] Stefan Maier,[†] Heng Wang,[+] G. Jeffrey Snyder,[+] Oliver Oeckler[*,‡]

[†]University of Munich (LMU), Department of Chemistry, Butenandtstraße 5-13 (D), 81377 Munich, Germany

[+]Materials Science, California Institute of Technology, 1200 E. California Blvd., Pasadena, CA 91125, USA

[‡]Leipzig University, Faculty of Chemistry and Mineralogy, IMKM, Scharnhorststraße 20, 04275 Leipzig, Germany

Table S1. Results from EDX analyses (SEM, 6 point analyses averaged per compound).

sample	atom-% (calculated)	atom-% (experimental)
$Ge_{0.53}Ag_{0.13}Sb_{0.27}\square_{0.07}Te_1$	Ge: 27.6; Ag: 6.9; Sb: 13.8; Te: 51.7	Ge: 29.0(12); Ag: 6.5(3); Sb: 14.6(4); Te: 49.9(7)
$Ge_{0.61}Ag_{0.11}Sb_{0.22}\square_{0.06}Te_1$	Ge: 31.4; Ag: 5.7; Sb: 11.4; Te: 51.4	Ge: 32.8(9); Ag: 5.2(2); Sb: 12.4(3); Te: 49.7(7)
$Ge_{0.77}Ag_{0.07}Sb_{0.13}\square_{0.03}Te_1$	Ge: 39.0; Ag: 3.4; Sb: 6.8; Te: 50.8	Ge: 39.9(4); Ag: 3.6(3); Sb: 6.9(3); Te: 49.8(6)

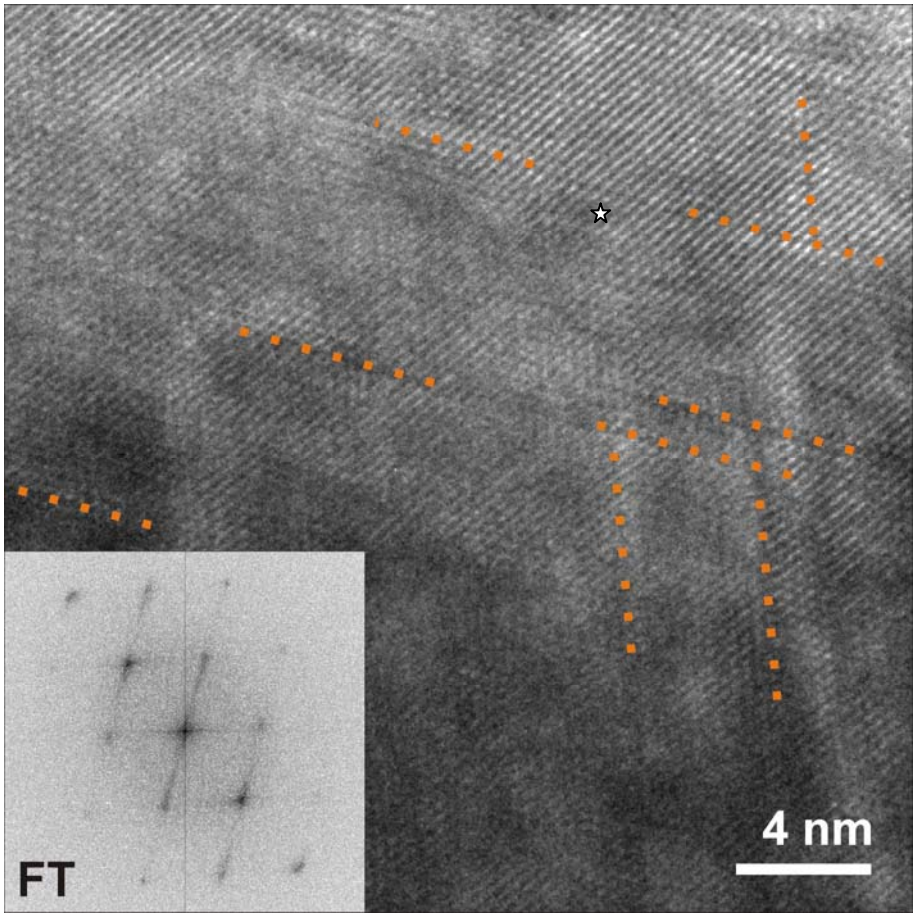

Figure S1. HRTEM image of quenched $Ge_{0.53}Ag_{0.13}Sb_{0.27}\square_{0.07}Te_1$ (zone axis [110]) with the corresponding Fourier transform (inset). Some vacancy layers are highlighted (dotted orange lines).

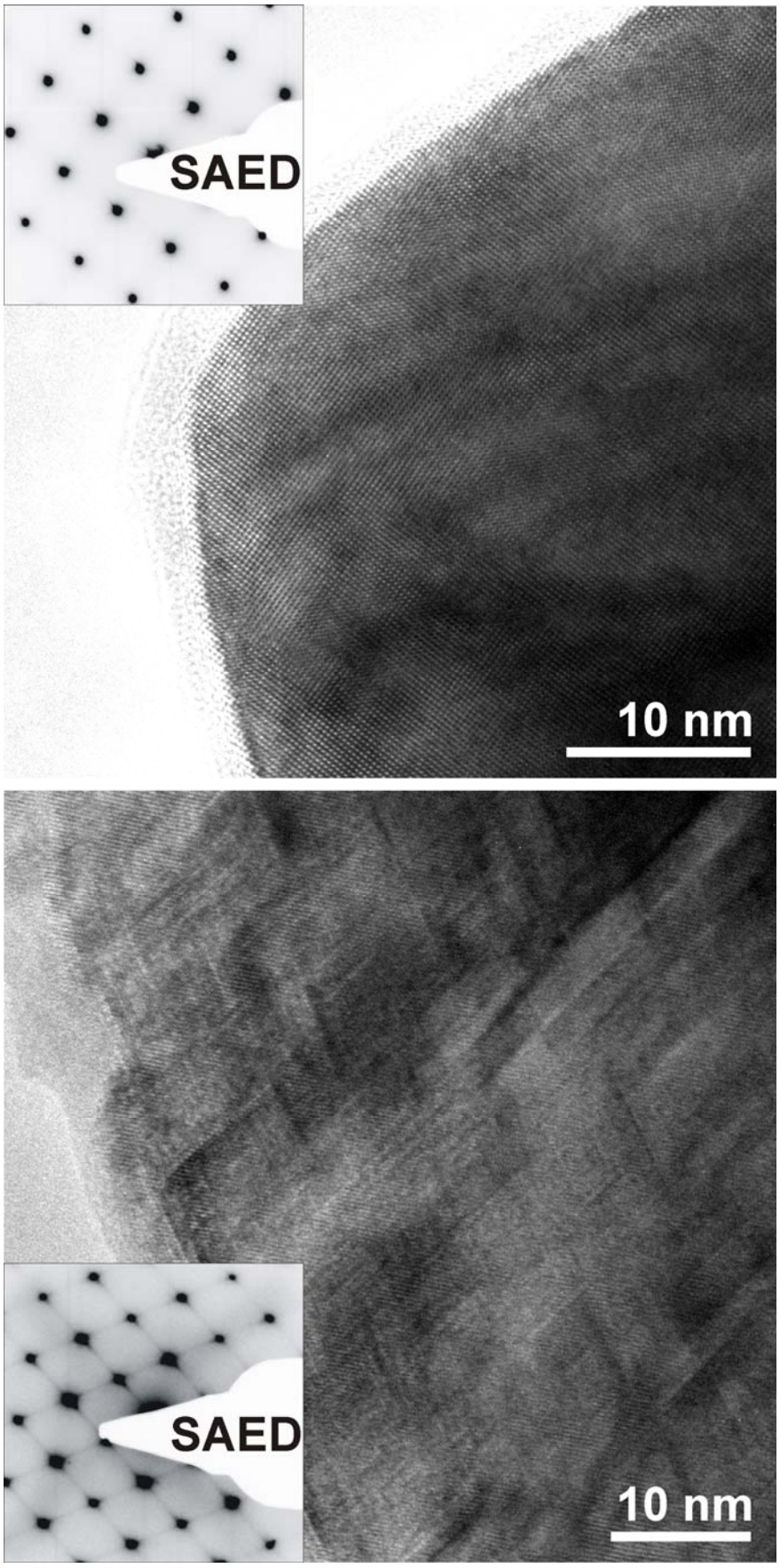

Figure S2. HRTEM images of quenched $Ge_{0.61}Ag_{0.11}Sb_{0.22}\square_{0.06}Te_1$ (top: zone axis [100], bottom: zone axis [110]) with the corresponding selected-area electron diffraction patterns of the crystallites (insets).

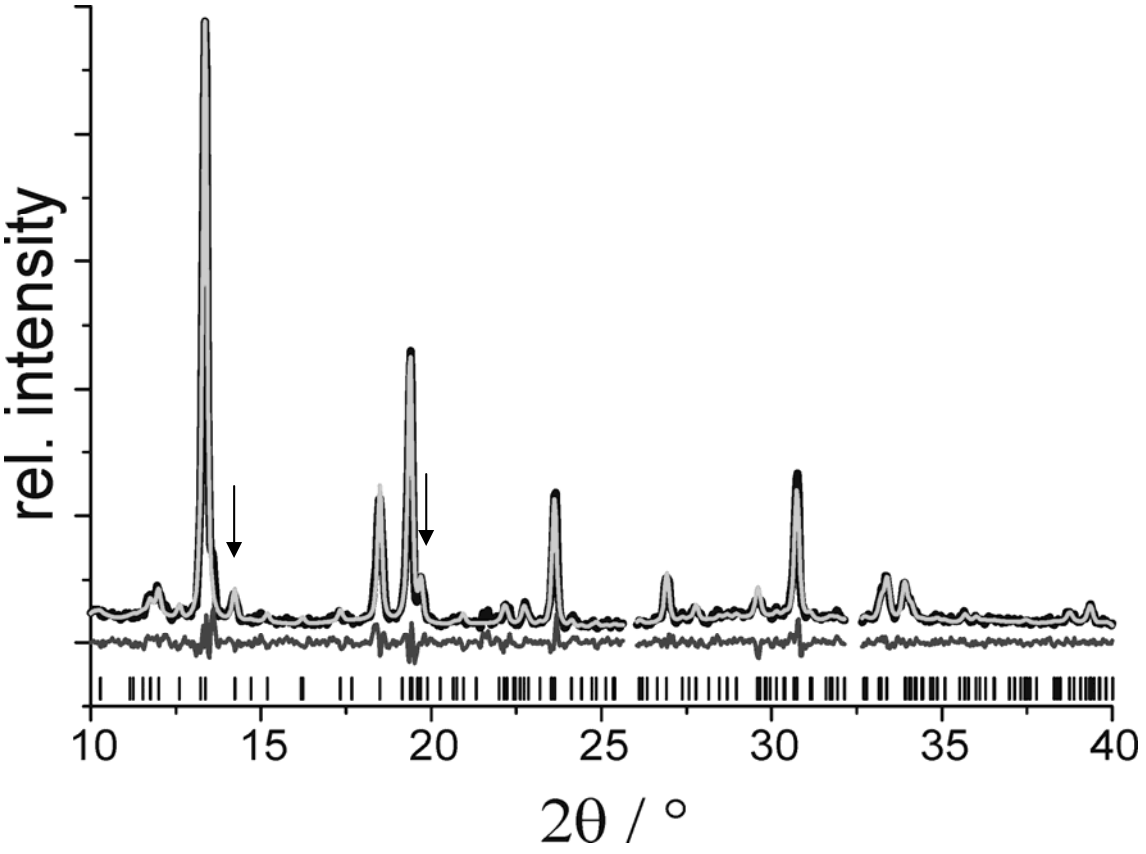

Figure S3. Rietveld refinement of $Ge_{0.53}Ag_{0.13}Sb_{0.27}\square_{0.07}Te_1$ in its trigonal long-periodically ordered layered 15*P*-$Ge_5As_2Te_8$ type structure (slowly cooled from the HT phase after the heating experiment): experimental (black) and calculated (light gray) powder diffraction patterns, difference plots (dark gray) and peak positions (black lines); space group $P\bar{3}m1$ (no. 164), a = 4.2136(3) Å; c = 27.711(4) Å, R_p = 0.0812, R_{wp} = 0.1087, R_{Bragg} = 0.0275. Reflections caused by the furnace at ca. 26° and 32.4° 2θ were excluded; arrows highlight the most significant reflections indicating long-range order (also visible and highlighted in the temperature-dependent PXRD patterns in the text).

Table S2. Atom positions, occupancy factors (s.o.f., atom distribution not refined), and displacement factors (B_{iso} in $Å^2$, common for cations and anions respectively) of $Ge_5As_2Te_8$ type $Ge_{0.53}Ag_{0.13}Sb_{0.27}\square_{0.07}Te_1$

sample	atom	x y z	s.o.f.	B_{iso}
$Ge_{0.53}Ag_{0.13}Sb_{0.27}\square_{0.07}Te_1$	Ge Ag Sb	0 0 0	4/7 1/7 2/7	1.6(3)
	Te	2/3 1/3 0.064(1)	1	0.8(2)
	Ge Ag Sb	1/3 2/3 0.136(1)	4/7 1/7 2/7	1.6(3)
	Te	0 0 0.191(1)	1	0.8(2)
	Ge Ag Sb	2/3 1/3 0.254(2)	4/7 1/7 2/7	1.6(3)
	Te	1/3 2/3 0.320(1)	1	0.8(2)
	Ge Ag Sb	0 0 0.392(2)	4/7 1/7 2/7	1.6(3)
	Te	2/3 1/3 0.447(1)	1	0.8(2)

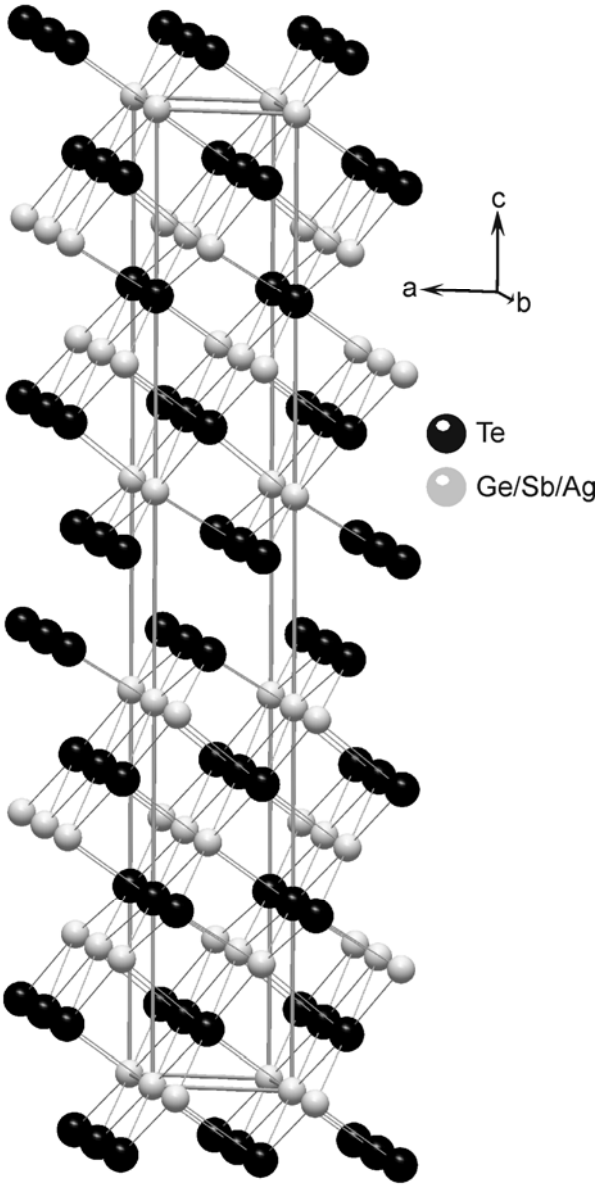

Figure S4. Crystal structure of 15*P*-type $Ge_{0.53}Ag_{0.13}Sb_{0.27}\square_{0.07}Te_1$, formed after slowly cooling the cubic high-temperature phase to room temperature.